

Contents lists available at ScienceDirect

# Cement and Concrete Composites

journal homepage: www.elsevier.com/locate/cemconcomp



# Nanosilica in-situ produced with sodium silicate as a performance enhancing additive for concretes

Xin Qian<sup>a</sup>, Heng Yang<sup>a</sup>, Jialai Wang<sup>b,\*</sup>, Yi Fang<sup>b,c</sup>, Liang Wang<sup>b,d</sup>, Peiyuan Chen<sup>d</sup>, Hongduo Zhao<sup>a</sup>

- a Key Laboratory of Infrastructure Durability and Operation Safety in Airfield of CAAC, Tongji University, Shanghai, 201804, PR China
- b Department of Civil, Construction, and Environmental Engineering, The University of Alabama, Tuscaloosa, AL, 35487, USA
- <sup>c</sup> College of Mechanics and Materials, Hohai University, Nanjing, Jiangsu, 211100, PR China
- d School of Civil Engineering and Architecture, Anhui University of Science and Technology, Huainan, Anhui, 232001, PR China

#### ARTICLE INFO

# Keywords: Nanosilica Tannic acid In-situ production Carbon emission Microstructure Compressive strength Sulfate resistance

#### ABSTRACT

This study proposes to use an in-situ produced nanosilica to enhance the performance of cement mortar. To this end, a two-step mixing method is developed. In Step I, low-cost sodium silicate and tannic acid (TA) solutions are mixed with the mixing water, in which TA can trigger the condensation of sodium silicate to produce porous silica nanoparticles and disperse the produced nanoparticles in the mixing water. The resulting mixing water with nanosilica is then directly used to mix cement mortar. Experimental results show that the compressive strength at 28d of the cement mortar produced by the proposed method is 35% higher than the one produced using the existing method. This strength improvement far exceeds what can be achieved by the ex-situ addition of nanosilica, which can be attributed to the fact that the in-situ produced nanosilica can significantly reduce the porosity of the cement paste, as revealed by the mercury intrusion porosimetry test. For the same reason, the produced cement mortar's resistance to sulfate attack is also enhanced by the proposed method. The proposed method is ready for large-scale field application in concrete since it overcomes all challenges facing the utilization of nanoparticles in concretes, such as high cost and difficult dispersion.

#### 1. Introduction

Many nanoparticles can be used as performance-enhancing additives (PEA) for Portland cement (PC)-based concrete, as shown in extensive studies [1]. After being added to the concrete at a small dose, this PEA can significantly improve the strength and durability of the concrete without using more cement. The carbon emission of the concrete can, therefore, be reduced since less cement clinker is needed for the concrete with the PEA to achieve a targeted strength.

These nanoparticles can enhance the compressive strength of the concrete by 5%–25% through a few mechanisms: a) providing nucleation seeding sites for hydration products to promote the hydration of PC, b) filling the pores in the concrete to produce a dense concrete with a lesser binder, c) reacting with hydration products to produce more binding materials, and 4) reinforcing hardened cement paste. Among many nanoparticles used in concrete, nano-silica is the most commonly used due to its exceptional pozzolanic reactivity [2–4]. In a study by Flores-Vivián, it was shown that the compressive strength of cement

mortar at both 1d and 28d was notably enhanced through the use of nanosilica synthesized via the sol-gel method, employing tetraethoxysilane (TEOS) as a precursor [5]. It is also reported that water glass can serve as a precursor for nanosilica production using the sol-gel method, leading to a substantial reduction in concrete porosity and a consequential improvement in its durability [6].

Although extensive studies have confirmed the great potential for nanoparticles as PEAs for concrete, their field applications in concrete structures are very few because of two major obstacles: low-cost efficiency and difficulty of uniform dispersion of nanoparticles [1,7,8]. The cost of nanoparticles itself is still 1000 times higher than the PC or other conventional raw materials employed for PC-based concrete [7]. Most nanoparticles cannot be easily dispersed because of high Van Der Waals interactions induced by their high specific surface area. Aggregation/agglomeration of nanoparticles is inevitable, leading to the formation of voids and weak zones in produced concrete [9]. Surfactants, ultrasonic energy, or chemical functionalization have been exploited to address this drawback [10,11], increasing the manufacturing cost of the

E-mail address: jwang@eng.ua.edu (J. Wang).

<sup>\*</sup> Corresponding author.

#### concrete.

Aiming to enable field application of nanoparticles as PEAs, this study proposes to in-situ produce silica nanoparticles through condensing low-cost, water-soluble sodium silicate (SS) by tannic acid (TA). This can be done by a two-step mixing method shown in Fig. 1. In Step I, both the SS and TA solutions are mixed with the mixing water. TA (Fig. 1(a)) is a water-soluble natural polyphenol and the world's thirdlargest class of plant components after cellulose and lignin [12]. With abundant reactive terminal phenolic hydroxyl groups, TA can trigger the condensation of SS to produce mesoporous nanosilica particles (Fig. 1(b) and (c)). More importantly, TA can disperse and stabilize the produced nanosilica in the mixing water. This is because TA can be coated on the surface of almost any substrate due to its abundant terminal phenolic hydroxyl groups (Fig. 1(a)) [13]. As a result, a layer of TA can be immediately coated onto the newly formed nanosilica particles, preventing the aggregation/agglomeration of the produced nanoparticles, as indicated in Fig. 1(b) [14]. In Step II, the mixing water with nanoparticles in-situ produced in Step I is added into the mix of the concrete as the mixing water without purification, filtering, and drying. This not only eliminates the cost and energy consumption associated with these processes but also avoids the difficult task of redispersing the produced nanoparticles, effectively eliminating two major barriers preventing field application of nanoparticles in concretes as PEAs. More importantly, residual TA in the suspension can enhance the mechanical performance of the produced concretes, as revealed by our previous research [15,16].

The proposed method can also be modified to produce calcium silicate hydrate (C–S–H) nanoparticles. C–S–H nanoparticles have been successfully used to seed the hydration of PC cement [17]. Co-precipitation from  $\text{Ca}(\text{NO}_3)_2$  and  $\text{Na}_2\text{SiO}_3$  in the presence of polycarboxylate (PCE) superplasticizers is a very popular way to produce C–S–H nanoparticles [18]. In this method, the superplasticizer has a similar function as TA: limiting the size and stabilizing the produced nanoparticles. The proposed method can be used to produce C–S–H nanoparticles by simply adding sodium silicate, calcium nitrate, and TA solutions into the mixing water in Step I.

In this study, a comprehensive experimental program was carried out to evaluate the potential of this in-situ produced nanosilica as a potent PEA for concrete. To this end, the performances of the cement mortars made with this PEA were compared with those made without it, as well as the ones made with ex-situ nanosilica. An array of characterization

tests were carried out to reveal the underlying mechanisms responsible for the performance enhancement.

#### 2. Materials and methods

#### 2.1. Materials

Type I/II PC was used to prepare cement paste and mortar samples. Its chemical composition is shown in Table 1. Lab-grade sodium silicate (SS, Na<sub>2</sub>SiO<sub>3</sub>) solution was used, containing 29.4 wt% of SiO<sub>2</sub>, 9.1 wt% of Na<sub>2</sub>O, and 61.5 wt% of water. The purities of TA and calcium nitrate tetrahydrate (CN, Ca(NO<sub>3</sub>)<sub>2</sub>·4H<sub>2</sub>O) are 98% and 99.9%, respectively. River sand with a bulk specific gravity of 2.70 and a water absorption capacity of 0.95% was used as the aggregate. The colloidal nano-silica (CNS) has a mean particle size of 20 nm and a solid content of 50%.

# 2.2. Sample preparation

Cement pastes and mortars were produced by the proposed two-step mixing method shown in Fig. 1. To make samples with in-situ nanosilica, TA was first fully dissolved in the mixing water in Step I. Then SS solution was then added and mixed with this TA solution. After aging for 30 min, the resulting suspension with in-situ produced nanosilica and residual TA was mixed with cement and sand to make paste/mortar samples in Step II. The same procedure was taken to prepare samples with in-situ produced C-S-H nanoparticles, except that CN was first dissolved in the mixing water before the addition of TA and SS in step I. The sample preparation was conducted under laboratory conditions at a room temperature of 23 °C. The morphologies of the in-situ produced nanosilica and C-S-H nanoparticles were analyzed with a transmission electron microscope (TEM). To do this, a drop of the produced nanoparticle suspension was deposited on a TEM grid. After the water was evaporated, TEM imaging was then carried out. The size of the produced nanosilica was determined by a laser diffraction particle size analyzer. The suspension of commercially available CNS was also examined for comparison.

A total of ten different mortar mixes were manufactured with mix design shown in Table 2: the Control group without any additive, the SS group in which only SS solution was added, the TA group in which only TA was added, the CNS group in which the PC was replaced by a certain amount of CNS, the TA+SS group with the nanosilica in-situ produced

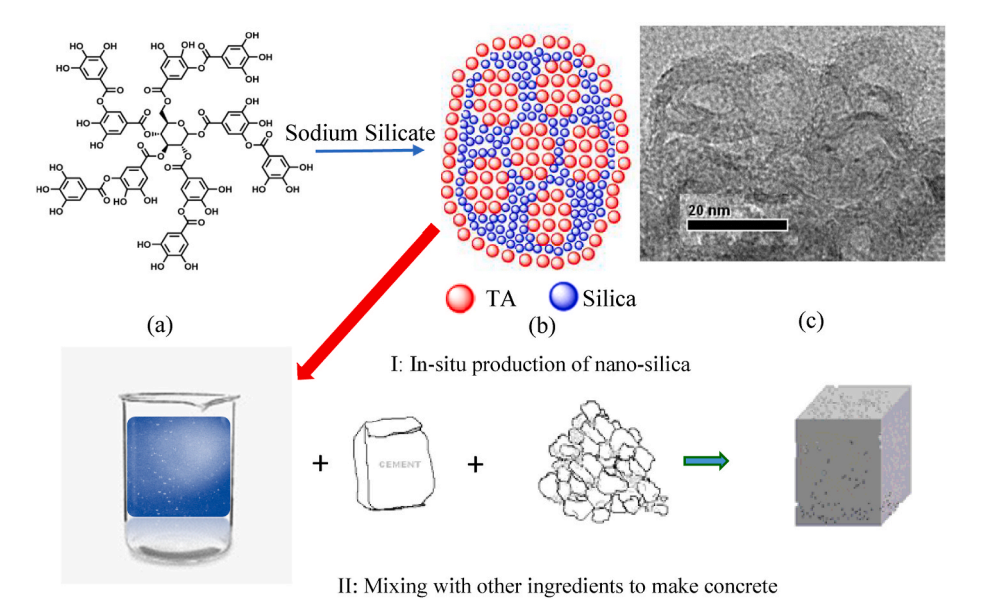


Fig. 1. In-situ production of porous nano-silica particles in fresh concrete: (a) chemical structure of TA; (b) TA stabilized hollow nano-silica nanoparticles; (c) TEM images of hollow nano-silica nanoparticles.

Table 1
Chemical compositions of PC (%).

Oxide Composition (%)	${ m SiO}_2$	CaO	$Al_2O_3$	$Fe_2O_3$	MgO	$Na_2O$	$K_2O$	LOI
Type I/II PC	22.93	64.04	4.68	2.41	3.38	0.23	0.76	0.82

**Table 2**Mix design for cement mortars produced with different methods (weight ratio).

Groups	Cement	Total Water <sup>a</sup>	River Ssand	SS (Solid)	CN	CNS (Solid)	TA
Control	1	0.5	2.52	_	_	-	_
SS	1	0.5	2.52	0.012	-	-	-
CN	1	0.5	2.52		0.0024	_	-
TA	1	0.5	2.52	-	-	_	0.002
CNS	0.99	0.5	2.52	-	-	0.01	_
SS+CN	0.99	0.5	2.52	0.012	0.0024	_	0.002
TA+SS	0.99	0.5	2.52	0.012	-	_	0.002
TA+SS+CN	0.99	0.5	2.52	0.012	0.0024	-	0.002
0.4 TA	1	0.5	2.52	-	-	-	0.004
0.4 TA+SS	0.99	0.5	2.52	0.012	-	-	0.004
0.4 TA+SS+CN	0.99	0.5	2.52	0.012	0.0024	-	0.004

<sup>&</sup>lt;sup>a</sup> For the groups with SS, total water = water + water from sodium silicate (solid content of sodium silicate: 38.5%) and for the group with CNS, total water = water + water from CNS (solid content of CNS: 50%).

by the proposed two-step mixing method, and the TA+SS+CN group with C-S-H produced by co-precipitation of SS and CN in TA solution in Step I. The contents of CNS, SS, and CN are 1%, 1.2%, and 0.24% in this analysis, respectively. Two concentrations of TA are employed in this study: 0.2% and 0.4%. All the percentages used in this study, if not specified, are given by the weight of the cement.

It should be mentioned that the mass of the SS solution is shown in Table 2, which includes 61.5% water. This amount of water was counted as part of the mixing water, and the amount of the mixing water in this table was reduced to maintain the same w/b ratio in the mortars with SS. The group CNS was prepared by adding 1 wt% CNS to the mortar mix, and the water from CNS itself was also considered mixing water.

## 2.3. Set time and flowability

In order to evaluate the effect of the proposed method on the setting times of cement paste, the initial and final setting times of produced cement pastes were determined using the Vicat needle based on ASTM C191 [19]. The workability of the fresh mortars was determined by the flow table test according to ASTM C1437 [20].

## 2.4. Isothermal calorimetry test

Isothermal calorimetry testing was carried out to investigate the effect of produced nanosilica on the hydration of the cement paste with a water-to-cement ratio of 0.5. I-Cal 4000HPC from Calmetrix Incorporation was employed in this test. The ratio between TA, SS, CNS, and CN is the same as in Table 2.

#### 2.5. Hydration products

The effect of the produced nanoparticles on the hydration products was evaluated with X-Ray Diffraction (XRD) and thermogravimetric analysis (TGA). The cement paste specimens in this test were prepared using the same mix as those used in the isothermal calorimetry test. After 3d and 28d of curing in a sealed bag, these specimens were pulverized to produce particles with a size smaller than 0.15 mm for testing. The specimens were dried at 60 °C for 24 h before the measurement to obtain the content of non-evaporation water.

# 2.6. Microstructure

A JEOL 7000 FE Scanning Electron Microscopy (SEM) was used to examine the microstructure of the cement paste samples. Five groups of paste samples with water to cement ratio of 0.5 were prepared: the Control group, the SS group, the TA group, the CNS group, and the TA+SS group. The contents of TA, SS, CN, and CNS are the same as those in Table 2. Their porosity and pore size distribution were also determined using mercury intrusion porosimetry (MIP).

# 2.7. Mechanical property test

The mortars produced with mixing proportions shown in Table 2 were prepared for the compressive test. These mortar samples were cast into  $50 \times 100$  mm cylinders. Their compressive strength was measured at ages of 3, 7, and 28d, respectively, based on ASTM C39. Capping pads were employed to minimize the impact of the surface roughness of the cylindrical sample on the measured compressive strength.

# 2.8. Durability test

The sulfate resistance of the cement mortars was tested on the mortar bars prepared based on ASTM C1012 with a dimension of  $25\times25\times275$  mm [21]. All groups employed the proportions detailed in Table 2, except for the sulfate resistance test, which required a water-to-cement ratio of 0.485 and a sand-to-cement ratio of 2.75, as per ASTMC1012. The dosage of TA and sodium silicate remained the same compared to the compressive strength and followability tests.

# 3. Results and discussions

# 3.1. Morphologies of produced nanoparticles

Fig. 2(a) shows a TEM image of nanoparticles produced by mixing SS and TA solutions after 30mins aging, which is the aggregate of many nanoparticles smaller than 40 nm. Fig. 2(b) shows that those small nanoparticles have a hollow core and a silica shell with a thickness of a few nanometers. The mechanism to induce this core-shell structure was proposed by Gao and Zharov [22]. This study confirms that porous nanosilica can be produced using low-cost sodium silicate and TA. Fig. 2 (c) should the particle size distribution of the produced nanoparticles measured by the laser diffraction method. It can be seen that the

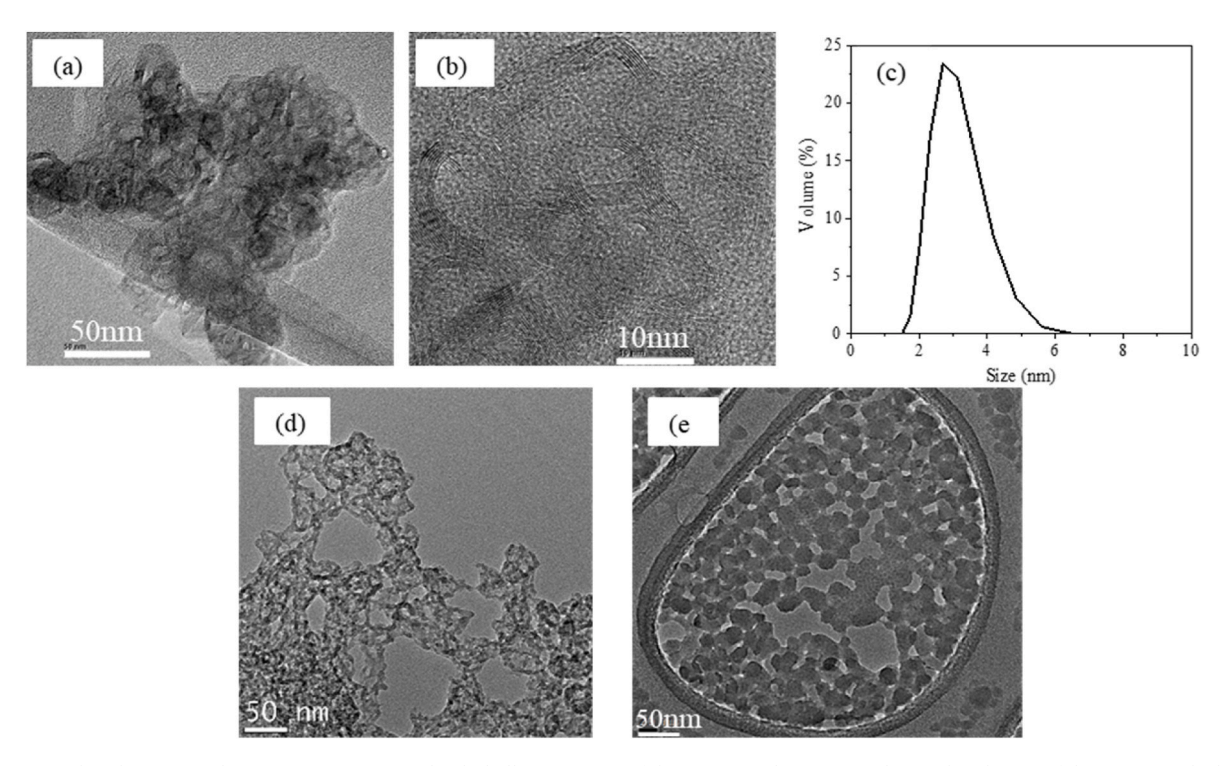


Fig. 2. In-situ produced nanoparticles: (a) SS-TA nanoparticle; (b) hollow structure of the nanoparticles; (c) particle size distribution of the nanoparticle determined by laser diffraction; (d) C–S–H nanoparticles in-situ produced by TA+SS+CN; (e) commercially available nanosilica.

measured size is much smaller than the size of the particle but very close to the thickness of the shell shown in Fig. 2(b). This suggests that the laser diffraction may only measure the thickness of the shell for hollow nanoparticles, which was also observed by Kong et al. [23]. Fig. 2(d) shows the TEM image of the nanoparticle produced by mixing CN, SS, and TA together. It can be seen that the morphology of the nanoparticle is very different from Fig. 2(a), indicating that the produced nanoparticle could be C-S-H after calcium ions were added. To further confirm this, these nanoparticles were filtered out after stirring the TA+SS+CN solution 30 min and the unreacted chemicals were removed through repeated washing with deionized water. The resulted precipitate was then dried at 60 °C for 12 h and examined by a scanning electron microscopy with energy dispersive X-ray spectroscopy (SEM/EDX). As shown in Fig. 3(a), the precipitate contains aggregations of nanoparticles with a size of less than 100 nm, as expected. The major element found in the spectra (Fig. 3(b)) indicates that C-S-H is the major mineral produced in our method. This is also confirmed by many existing studies, which suggest that C-S-H nanoparticles can be produced by the reaction between SS and CN [24] Fig. 2(e) shows the morphology of the commercially available colloidal nanosilica particles.

# 3.2. Set time and workability

Table 3 shows the set time results of the cement pastes prepared with different methods. The addition of TA can significantly increase their setting times, as expected, since the TA can retard the hydration of cement paste [25]. The utilization of CNS greatly reduced the setting time of cement paste, as expected. The addition of SS slightly reduced both the initial and final set times in comparison to those of the Control

 $\begin{tabular}{ll} \textbf{Table 3} \\ Effect of the in-situ produced bio-nano particles on the setting time of the cement pastes. \\ \end{tabular}$ 

Group	Initial Set(min)	Final Set(min)
Control	152	243
SS	141	235
TA	283	441
CNS	109	203
TA+SS	262	432
TA+SS+CN	95	189

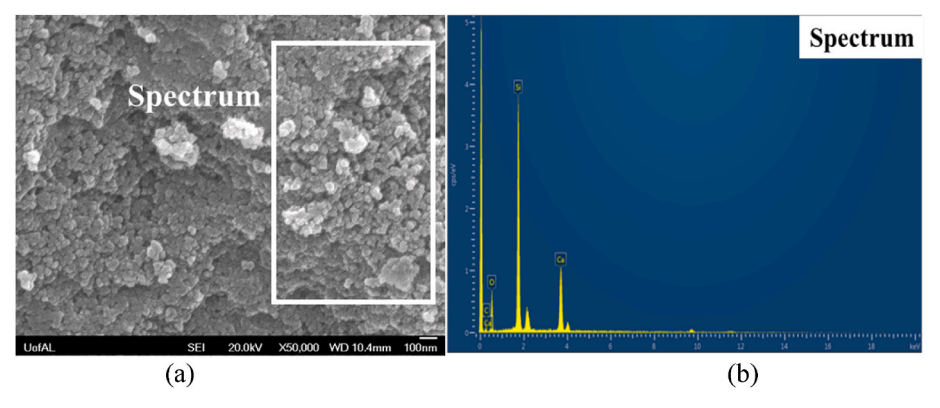


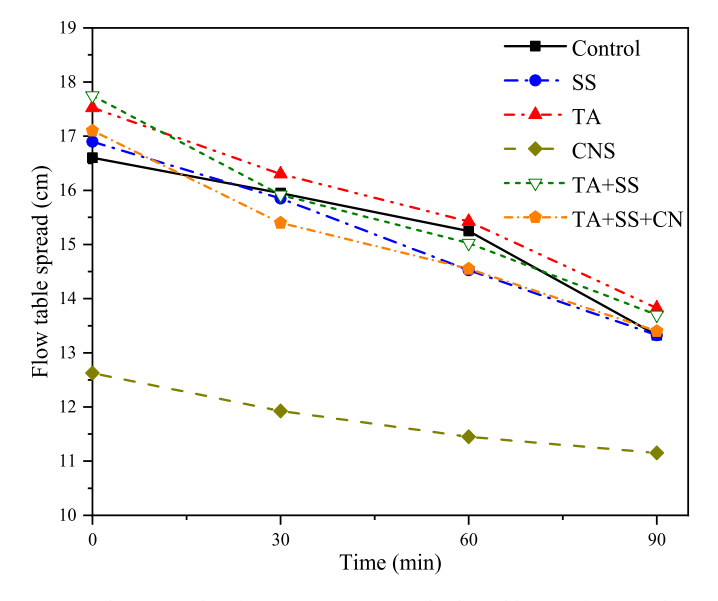
Fig. 3. Representative SEM images of produced C-S-H nanoparticles: (a) aggregation of C-S-H nanoparticles; (b) corresponding EDX spectrum of (a).

group, which can be attributed to the acceleration effect of sodium ions by increasing the pH value [26]. Adding the nanosilica in-situ produced by mixing TA and SS (TA+SS in Table 3) in mixing water can only partially mitigate the retarding effect of TA. This is expected since TA in the suspension was not filtered, retarding the hydration of the cement. This retarding effect can be fully eliminated if CN is also added. As shown in Table 3, both initial and final set times of the TA+SS+CN sample were drastically reduced to even shorter than those of the Control group. This can be attributed to CN, which can accelerate the hydration of PC, especially at low temperatures [27]. Table 3 suggests that set times of concrete can be adjusted by the ratio between the retarder TA and the accelerator CN.

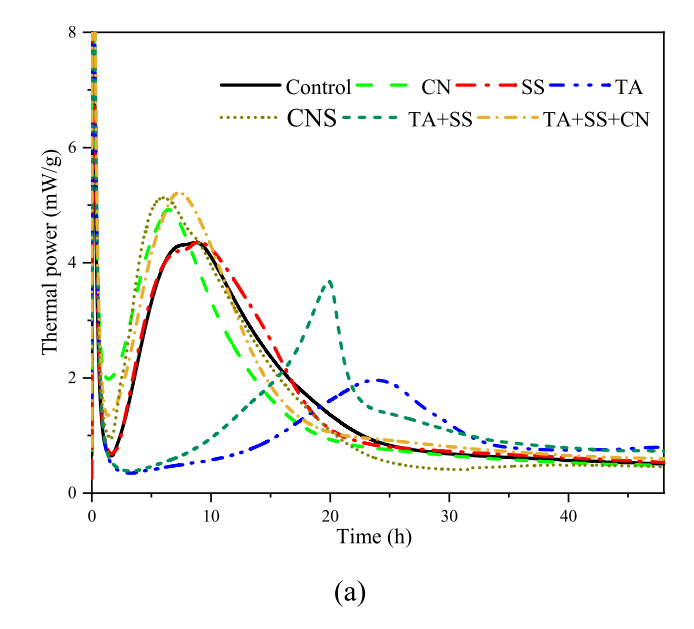
Fig. 4 compares the flowabilities of the cement mortars produced with different methods. Among all samples, the CNS mortar had the lowest flowability, suggesting that adding CNS can significantly reduce the workability of the cement mortar due to the large surface area of the nanosilica. The flowability of the cement mortar was increased by adding TA because TA can be adsorbed on the surface of cement particles, making the surface of cement particles negatively charged. This creates static repulsion between cement particles, leading to better workability. For this reason, the flowabilities of the TA+SS and TA+SS+CN samples were also higher than that of the control mortar. This is an extra benefit of using the in-situ produced nanoparticles without filtering out the TA out. The flowabilities of all these samples were reduced with time due to the hydration of the cement. Among them, the flowabilities of TA+SS+CN and SS samples decreased at higher rates than other samples, indicating the hydration of these two samples was accelerated. This is in agreement with the observation on set times shown in Table 3.

#### 3.3. Hydration heat

Isothermal calorimetry was employed to investigate the effect of the in-situ produced nanosilica on the hydration of cement, as shown in Fig. 5. As expected, the addition of in-situ produced nanosilica can retard the hydration of the cement, as revealed by the TA+SS curve in Fig. 5(a) due to the presence of TA in the suspension. The retarding effect of TA can be seen more clearly in the TA sample, in which the appearance of the peak corresponding to C<sub>3</sub>S hydration was delayed to almost 24 h, and the peak thermal power was reduced by more than half. This retarding effect was partially mitigated by the in-situ produced nanosilica through its seeding effect [3,28–30]. The retarding effect of



**Fig. 4.** Flow spreads of cement mortars with the addition of TA/SS bionano particles.



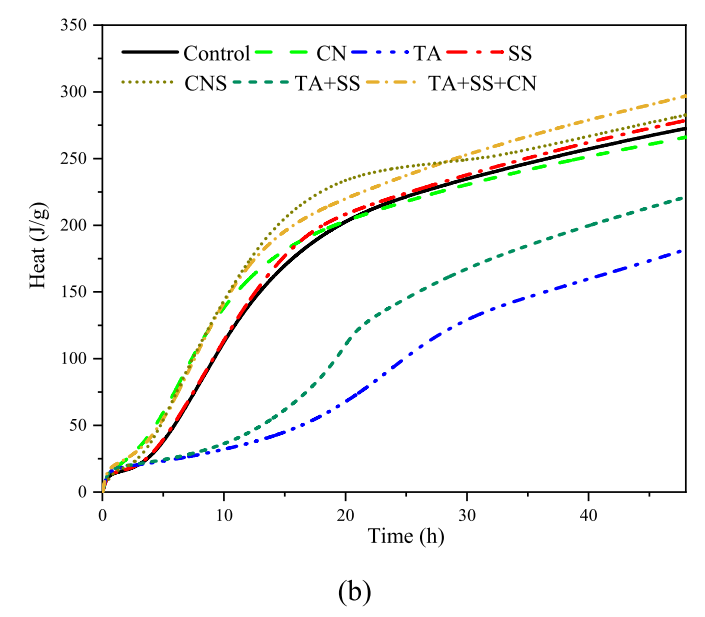


**Fig. 5.** Comparison of hydration heat of the cement pastes prepared with various additives:(a) rate of hydration; (b) cumulative heat of hydration.

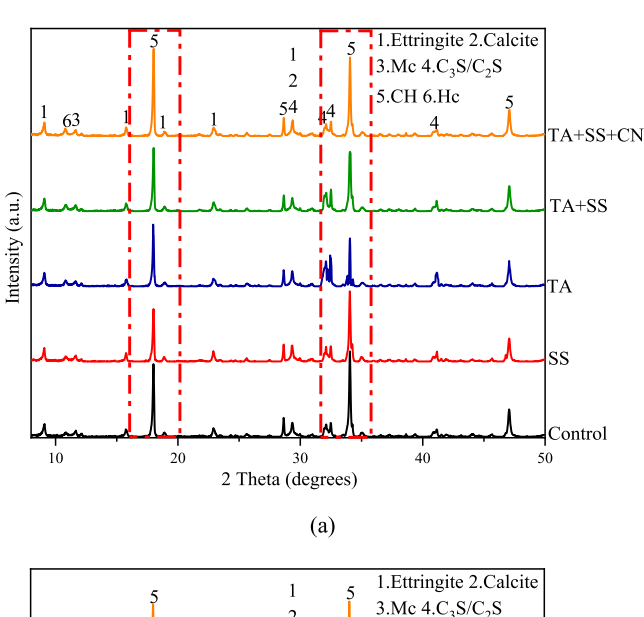
TA was fully eliminated by adding the in-situ produced C–S–H nanoparticles (TA+SS+CN curve in Fig. 5(a)). Compared with the control sample, this sample has a short induction period and higher peak thermal power, suggesting that the hydration of the cement was accelerated. The major reason responsible for this acceleration can be attributed to the accelerating effect of CN, which is revealed by the curve of the CN sample shown in Fig. 5(a). Similar to CN, CNS can also accelerate the hydration of cement [31,32], which agrees well with the results in set time measurement (Table 3).

Fig. 5(b) compares the total heat released from the hydration of the cement pastes. Both the SS and CN can slightly affect the total heat released during the hydration. The addition of TA reduced the accumulated hydration heat of the cement paste at 72 h by 23%. The use of nanosilica in-situ produced by SS and TA mitigated this retarding effect such that the reduction of accumulated hydration heat at 72 h was reduced to 11%. These reductions in accumulated hydration heat will diminish at late age since the thermal powers of TA and TA+SS pastes are higher after the deceleration period, as shown in Fig. 5(a). The

TA+SS+CN paste generates the highest hydration heat among all the groups, primarily due to the additional seeding sites provided by the C–S–H nanoparticles and the acceleration effect of CN. Similar to the case of set time, this figure indicates that the hydration speed of the cement can be tuned using SS, TA, and CN. By adjusting the ratio among SS, TA, and CN, various demands on the hydration rate of the cement can be satisfied.

## 3.4. Hydration products

Fig. 6(a) presents XRD spectra of the paste samples at 3d. Typical hydration products such as calcium hydroxide (CH), C–S–H gel, and ettringite are marked in these spectra. It can be seen that no new mineral is produced by the addition of TA. The peaks of  $C_2S$  and  $C_3S$  of the sample prepared with TA are the highest among all tested samples due to the retarding effect of TA on the hydration of  $C_2S$  and  $C_3S$  at early age. The peaks of CH in the TA+SS sample are higher than that of the TA sample, indicating the retarding effect of TA can be alleviated by the insitu produced nanosilica. The combination of SS, TA, and CN can fully eliminate the retarding effect of TA on cement hydration, as the TA+SS+CN sample has the highest peaks of CH. All these features agree well with the results of hydration heat measurement. Our previous research found that the addition of TA can affect the growth of CH crystals [33]. Fig. 6(a) shows that the peak at 2-theta of 22° is higher



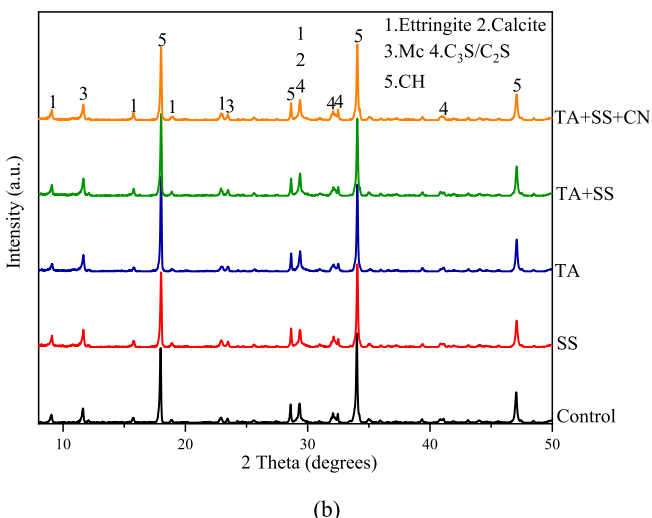


Fig. 6. XRD patterns of cement paste produced with different methods at (a) 3d; (b) 28d.

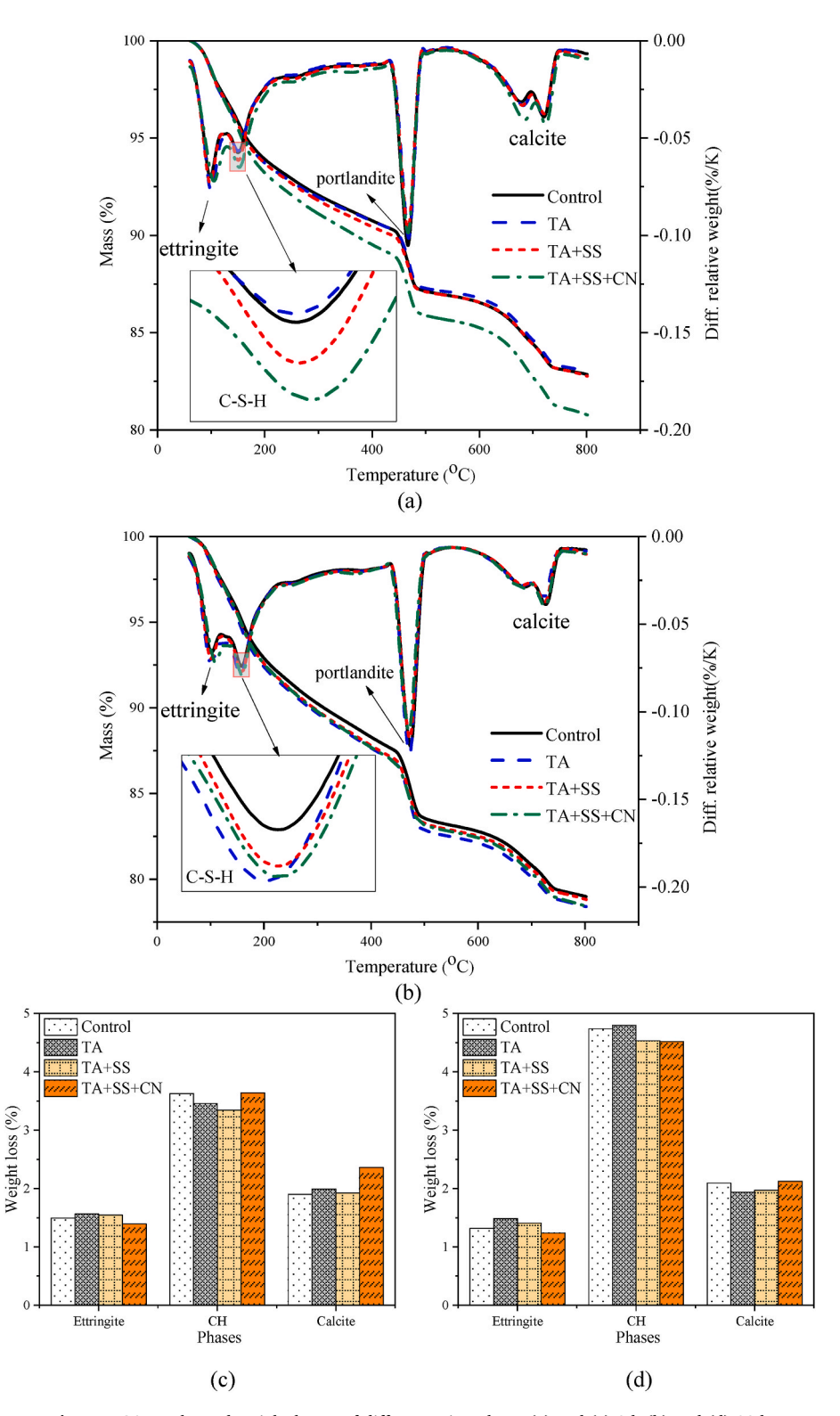
than the peak at 2-theta of  $40^{\circ}$  in all the specimens prepared with TA. This means that more CH crystal orientated with their c-axis was produced by the addition of TA. The retarding effect of TA can not be observed at 28d. As shown in Fig. 6(b), the spectra of all samples are very similar. Particularly, the peak corresponding to CH in the specimens prepared with TA is slightly higher than those of other samples, as shown in Fig. 6(b). This suggests that TA can promote the hydration of the cement at late age. The spectra of the sample prepared with SS are almost identical to the control one. It means the addition of SS has little influence on the hydration product.

TGA was employed to analyze the hydration products quantitatively, as shown in Fig. 7. It is generally believed that the dehydration of hydrates like C-S-H gel and ettringite causes weight loss between 100 and 200 °C [34], and the ettringite tends to decompose below 120 °C [35]. Since TA can form a complex with calcium, the dehydration of C-S-H was employed to compare the effect of in-situ produced nanoparticles and CNS on the hydration products, as shown in the enlarged areas in Fig. 7(a) and (b). It can be seen that the paste with TA produced the lowest amount of C-S-H gel at 3d, clearly due to the retarding effect of TA. The addition of nanosilica in-situ produced by TA and SS mitigates the retarding effect of TA and produces more C-S-H gel in comparison with the control sample. This can be attributed to the pozzolanic reaction between the nanosilica and CH, which can produce more C-S-H in the TA+SS sample. The use of calcium nitrate further increases the content of C-S-H gel, which is resulted from accelerated hydration. At 28d, the sample with TA appears to have the highest content of C-S-H, suggesting that TA promotes the hydration of the cement at late age. This agrees well with the results obtained from the XRD analysis. At this age, C-S-H contents in both TA+SS and TA+SS+CN exceed that in the control sample, as expected.

Fig. 7(c) and (d) show the calculated weight loss of different minerals obtained from TGA. At 3d, adding TA reduced the CH content in the TA sample compared with the control one due to the retarding effect of TA. Although this retarding effect can be partially mitigated in the TA+SS sample, CH content in this sample is even lower. This reduction of CH content was induced by the pozzolanic reaction between CH and nanosilica, which consumes some CH to produce more C-S-H gel. Due to the acceleration effect of CN, the CH content in the TA+SS+CN sample is much higher in comparison with the other two samples. At 28d, CH content in the TA sample caught up with the control sample since the retarding effect was completely diminished at this age, as revealed by its XRD spectrum and content of C-S-H at this age. Similar to 3d, the CH content in the TA+SS sample at 28d is still lower than the control group, obviously due to the pozzolanic reaction between the in-situ produced nanosilica and CH. The CH content in the TA+SS+CN sample at this age is also lower than the one of the control sample. This can be induced by two reasons: a) the acceleration effect of CN is less pronounced at this age, and b) some CH is consumed by the reaction between unreacted SS and CH.

Slightly more ettringite was found in the TA and the TA+SS pastes at 3d because of the presence of TA, which hindered the conversion from ettringite to AFm. This can be seen more clearly at 28d. At this age, ettringite content in the TA paste was almost identical to that at 3d, while ettringite contents in all other pastes were reduced. Fig. 7(c) also shows that the content of calcite in the TA+SS+CN paste at 3d is significantly higher than that in other samples. This indicates that not all calcium nitrate reacted with SS, leading to more calcium ions in the paste. These calcium ions can be easily carbonated, producing more calcite in the produced cement paste.

The hydration degree of the cement paste was quantitively characterized by calculating the content of non-evaporable water in the pastes, and the results are shown in Table 4. It should be mentioned that this measurement can also include weight loss due to the decomposition of the calcium tannate, a complex formed between TA and calcium ions or residual TA in the paste. Nevertheless, non-evaporable water content at 3d clearly shows that TA retarded and TA+SS+CN accelerated the



 $\textbf{Fig. 7.} \ \ \textbf{TGA results and weight losses of different minerals at: (a) and (c) 3d; (b) and (d) 28d.$ 

hydration of the cement pastes at 3d. At 28d, all paste samples had similar contents of non-evaporable water, suggesting that the effect of these additives on the hydration of the cement diminished at 28d.

## 3.5. Microstructure

Fig. 8 shows the SEM images of the representative microstructures of the cement pastes at 28d. As shown in Fig. 8(a), hexagonal CH crystals

were randomly deposited in the control paste sample. After adding CNS, the microstructure of the paste becomes denser, as shown in Fig. 8(b). Similarly, the denser microstructure is achieved by adding TA, as shown in Fig. 8(c). Particularly, CH in this paste is much more stacked, as shown in Fig. 8(c). This is because the c-axis oriented CH, as revealed in XRD analysis, tends to form new CH crystals onto the existing CH surface (Fig. 8(d)). This stacked microstructure of CH can enhance its stability in a corrosive environment. For the same reason, a similar structure of CH

**Table 4**Effect of the proposed method on the non-evaporation water content (%) of the cement pastes.

Sample	Age		
	3d	28d	
Control	17.1	21.0	
TA	17.0	21.6	
TA+SS	17.2	21.2	
TA+SS+CN	19.2	21.6	

can be found in the TA+SS paste, as revealed by Fig. 8(e). This phenomenon is not observed on the CNS paste since TA is not available. Abundant nanoparticles around 20 nm–30 nm are found in the TA+SS paste, as shown in Fig. 8(f). These nanoparticles were also reported in a previous study [14], which was presumably a calcium-TA complex produced by the reaction between calcium ions and TA. This figure clearly shows that the effects of ex-situ and in-situ produced nanosilica on the microstructure of the cement mortar are very different. In-situ produced nanosilica can lead to denser microstructure and more oriented growth of CH.

MIP tests were carried out on these pastes to further confirm the observation from SEM shown in Fig. 8, and the results are shown in Fig. 9. It can be seen that the addition of in-situ produced nanosilica can significantly reduce the total porosity of produced cement paste, from 29.7% of the control sample to 24.5% of the TA+SS sample, as shown in Fig. 9(b). The addition of TA also reduced the porosity of the cement paste to 25.8%. This can be partially attributed to the promoted hydration of cement by the TA at a late age, as revealed by Figs. 6 and 7. Another possible reason is the nanoparticles in-situ produced during the hydration of the cement under the influence of TA, as shown in Fig. 8(f) and a previous study [15].

Fig. 9(a) reveals a distinct feature of the pore size distribution of the pastes with the presence of TA: capillary pores with a size of 50 nm are drastically reduced in comparison with other samples. This can be attributed to the nucleation and filler effects of those produced nanoparticles with a size smaller than 30 nm in Fig. 8(f). Although pores in this region do not strongly affect the strength of the mortar, they play critical roles in the long-term durability of the concrete because both the drying shrinkage and creep of concrete are determined by these pores. Ex-situ addition of CNS can only slightly reduce the nanopores in the produced cement paste. This is because most pre-fabricated nanosilica

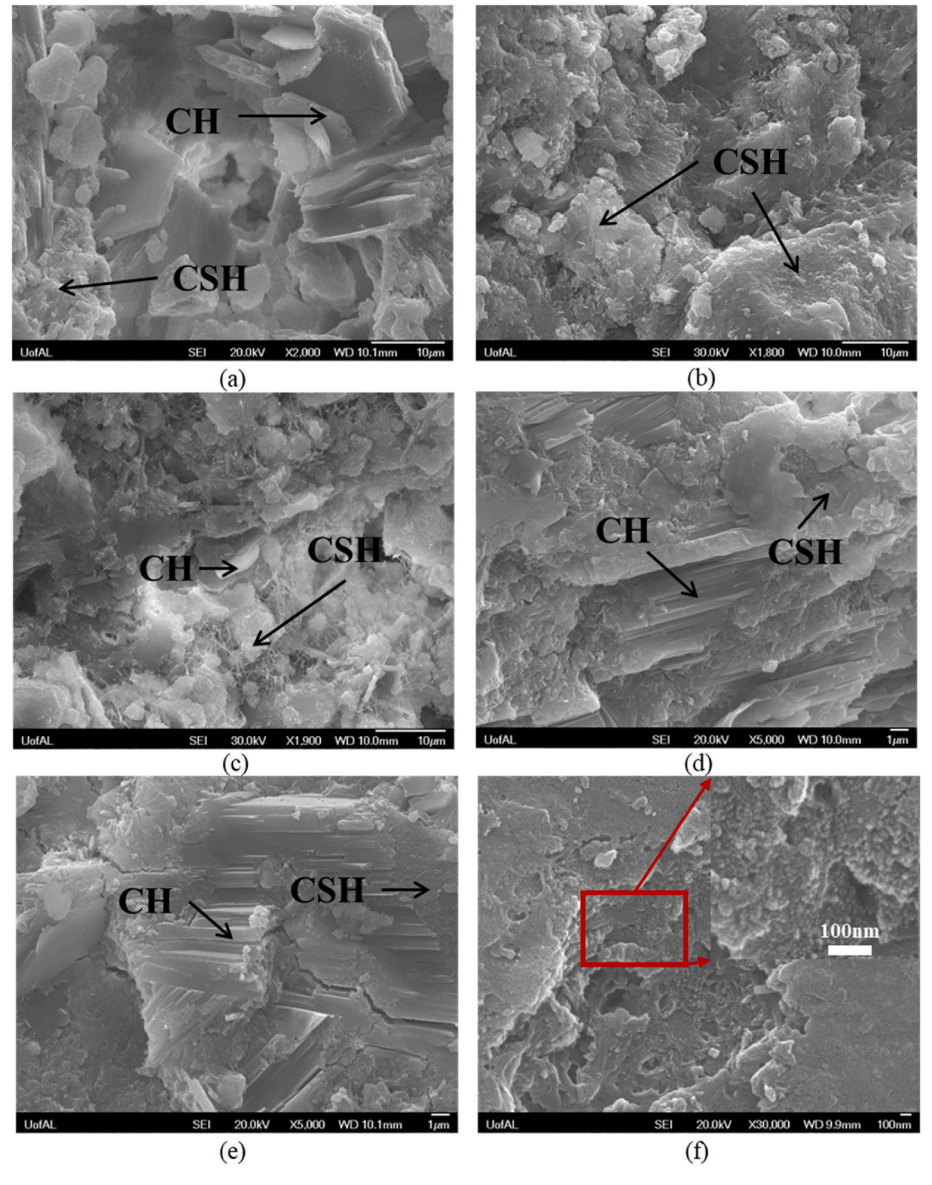
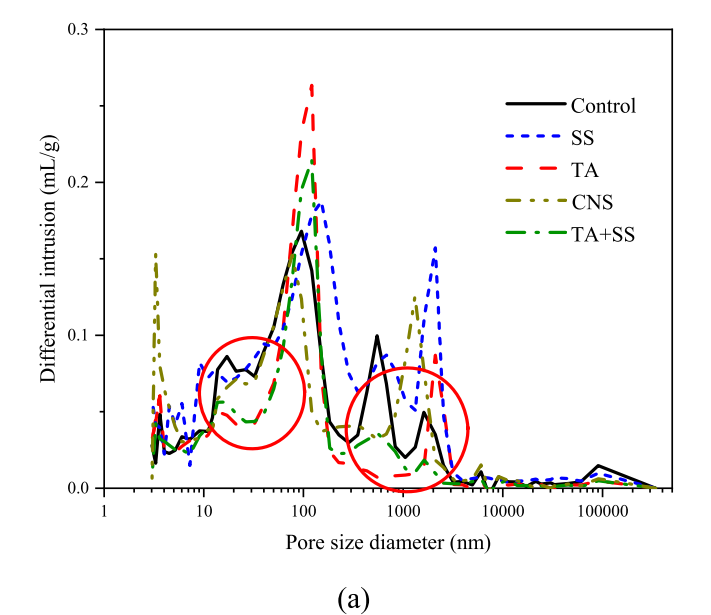
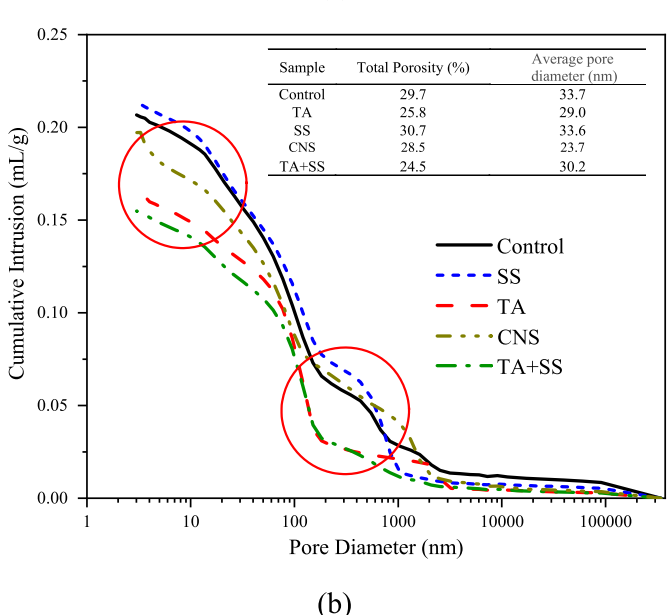


Fig. 8. SEM images of cement pastes at 28d: (a)Control; (b) CNS; (c) and (d) TA; (e) and (f) TA+SS.



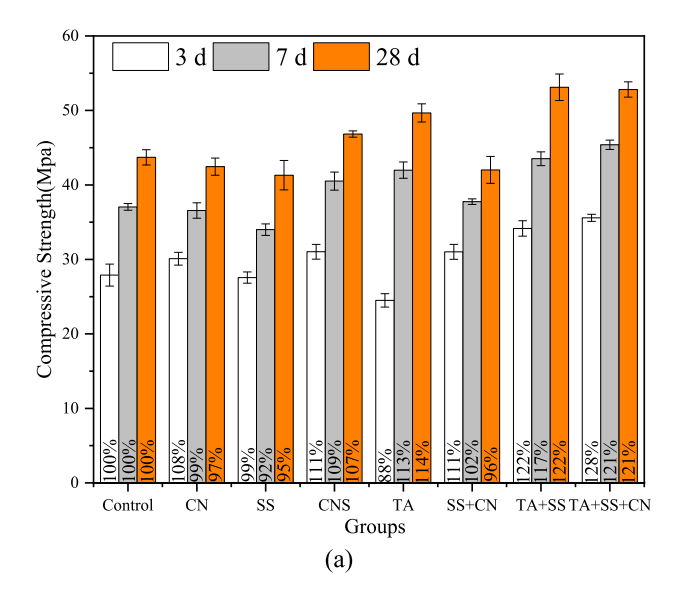


**Fig. 9.** The pore structure of cement pastes with and without using in-situ produced nanosilica at 28d: (a) differential pore-size distribution; (b) cumulative pore volume.

immediately re-agglomerated in the fresh cement paste due to their high van der Waals force [35]. Fig. 9 also shows that large capillary pores of around 1  $\mu m$  were significantly reduced by adding the in-situ produced nanosilica, which can be attributed to the improved workability of the produced cement paste, as shown in Fig. 4. These results are in good agreement with the observation by SEM, which reveals that denser microstructure was induced by the addition of the in-situ produced nanosilica. In addition, Fig. 9 suggests that the addition of SS into cement paste can actually increase the porosity of the paste, induced by the slight acceleration effect of extra sodium.

# 3.6. Mechanical properties

The effect of the in-situ produced nanosilica on the compressive strength of the produced cement mortar is revealed in Fig. 10, which compares the compressive strengths of the cement mortars with the mix design detailed in Table 2. Compared with the control sample, the



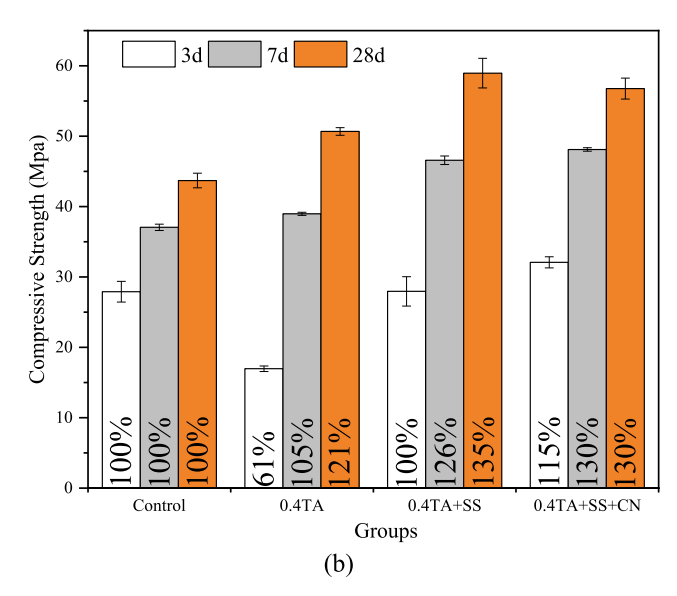


Fig. 10. Compressive strength of cement mortars prepared with different dosages of TA: (a)0.2%; (b) 0.4%.

compressive strengths of the mortar with the proposed nanosilica were enhanced by 22%, 17%, and 22% at 3d, 7d, and 28d, respectively, as revealed by the TA+SS sample in Fig. 10. This is not surprising since its total porosity is 5.2% lower than the porosity of the control sample, as shown in Fig. 9. This improvement on strength far exceeds that reached by the ex-situ addition of nanosilica. The compressive strength of the CNS mortar surpasses that of the control sample at 3d, 7d, and 28d by 11%, 9%, and 7%, even though the amount of the solid nanosilica in this mortar (1% by weight of the cement) is more than the solid nanosilica in-situ produced in the TA+SS sample (0.4%). The much better performance of the in-situ produced nanosilica over the ex-situ one can be attributed to their capacities to densify the microstructure of the produced cement mortar. As revealed by Fig. 8, more reduction in the porosity of the mortar was induced by the in-situ produced nanosilica than by the ex-situ CNS. Particularly, in-situ produced nanosilica can fill the nanopores smaller than 50 nm, which cannot be done by the ex-situ CNS.

Fig. 10 also shows the compressive strengths of the mortar made by adding only TA or SS. When only SS solution was added, the compressive strength of the produced mortar was slightly reduced for all ages due to

the poorer microstructure of the mortar induced by the addition of SS, as revealed by Fig. 9. Significant reduction in the compressive strength at early age (3d) was observed for the sample added with TA. This is expected due to the strong retarding effect of the TA, as confirmed by the calorimetry resting result shown in Fig. 5. This retarding effect diminished after 7d, and the compressive strength of the mortar sample exceeded that of the control one by 13% and 14% at 7d and 28d, respectively. This agrees with our previous study [25]. The much better performance of the TA+SS mortar over SS and TA mortars clearly demonstrates the synergy between the TA and SS, which not only produces the nanosilica to mitigate the retarding effect of TA but also disperses the produced nanosilica such that much better microstructure can be reached, as revealed by MIP study shown in Fig. 9.

Similar strength improvement can also be achieved by adding in-situ produced C–S–H particles. Fig. 10 shows that the compressive strength of the TA+SS+CN mortar at 3d is 28% higher than the control one. This is not surprising since the hydration of the cement was accelerated by the addition of the CN. This can be confirmed by the compressive strength at 3d of the CN mortar, which was improved by 8% by adding CN only. However, only adding CN failed to improve the compressive strengths of the mortar at the late ages (7d and 28d). This agrees with existing studies, in which CN can mainly improve the early-age strength of PC-based concrete but with impaired late-age strength [31]. As a comparison, the compressive strengths of the TA+SS+CN at 7d and 28d are still 21% higher than the control one, indicating the necessity of C–S–H nanoparticles to enhance the performance of the mortar.

However, adding C-S-H nanoparticles produced with SS and CN in the mixing water without TA dispersion not only enhanced the early age (3d and 7d) strengths but reduced the strength of the mortar at late age (28d), as revealed by the SS+CN mortar in Fig. 10(a). This agrees well with many existing studies, which suggest that C-S-H seeding failed to improve long-term strength, even though a large increase in compressive strength at an early age can be obtained [36]. Van Damme indicated that C-S-H seeding could not increase the average density of the hydrated paste [36]. He further stated that "changing the mesoscale structure can only have a second-order influence on the final properties. The first-order parameter remains the relative volume of hydrates". Over 20% improvements in the compressive strength at 28d achieved by both the TA+SS and TA+SS+CN mortars suggest that this limitation of existing C-S-H seeding technology can be overcome by the proposed method. Particularly, similar strength improvement at 28d was achieved by the TA+SS+CN sample. This implies that the strength development rate of the mortar can be fully controlled by adjusting the content of CN without losing the late age strength. This technique can also be used to control the release rate of the hydration heat, which is important to control the crack of concrete at an early age [37].

Fig. 10(a) shows that TA plays a critical role in the present technology. This can be further confirmed by Fig. 10(b), in which the content of TA was increased from 0.2% in Fig. 10(a) to 0.4% by the weight of cement. With more TA, higher strength improvement at late ages (7d and 28d) for mortars made TA+SS and TA+SS+CN added. 26% and 35% strength improvement were achieved by the mortar with in-situ produced nanosilica at 7d and 28d, respectively. If no SS or CN is added, the strong retarding effect of TA can significantly retard the hydration of the cement mortar at an early age, as revealed by a 39% reduction of the compressive strength at 3d of the mortar with 0.4% TA. Clearly, the seeding effect of the in-situ produced nanoparticle can mitigate the retarding effect of the TA.

## 3.7. Durability

As shown in Fig. 8, CH crystals are densely packed to form multilayers in the sample produced with TA. It can be expected that their chemical stability in an aggressive environment can be significantly improved. Together with densified microstructure, the proposed method can lead to higher resistance to chemical attack. This can be partially confirmed by Fig. 11, which shows the expansion of cement mortar bars prepared with the mix detailed in Table 2 immersed in the sulfate solution. The cement mortar prepared with only TA exhibited the lowest expansion among all four groups, revealing the unique ability of TA to enhance the chemical stability of the hydration products of cement. Compared with the TA sample, TA+SS mortar experienced larger expansion because some TA was trapped in the porous nanosilica. Nevertheless, this expansion is still much lower than that of the Control and SS mortars, clearly suggesting that the nanosilica in-situ produced by TA and SS can be conveniently used as a PEA for concrete to enhance both the strength and durability.

#### 4. Conclusions

This study demonstrates that porous nanosilica can be in-situ produced by simply mixing low-cost sodium silicate solution with tannic acid. This nanosilica can be used as a PEA for concrete. Both the compressive strength and durability of the mortar are significantly enhanced by this PEA since the in-situ produced nanosilica significantly densifies the microstructure of hydration products. Similar strength enhancement cannot be achieved using ex-situ nanosilica. Particularly, over 35% improvement on the compressive strength of the cement mortar at 28d was reached by the proposed nanosilica, eliminating the limitation of existing C–S–H seeding technology, which fails to enhance the late age strength. It is important to enhance the late age strength of the concrete since much less cement is needed to reach a specific strength, leading to a much lower carbon footprint of the concrete.

The in-situ produced nanosilica is well dispersed in the mixing water and can be directly added into concrete, eliminating all cost that makes the existing nanoparticles expensive, including purification, filtration, drying, packing, storage, dispersion, and shipping. In addition, this study provides an effective way to control hydration kinetics and strength development of concrete. Particularly, the hydration heat can be reduced by the proposed PEA without sacrificing early-age strength. Therefore, the proposed PEA can also be used to mitigate the temperature rise in concrete at the early age.

## **Declaration of competing interest**

The authors declare the following financial interests/personal relationships which may be considered as potential competing interests: Jialai Wang reports financial support was provided by US NSF. Jialai Wang has patent issued to The University of Alabama.

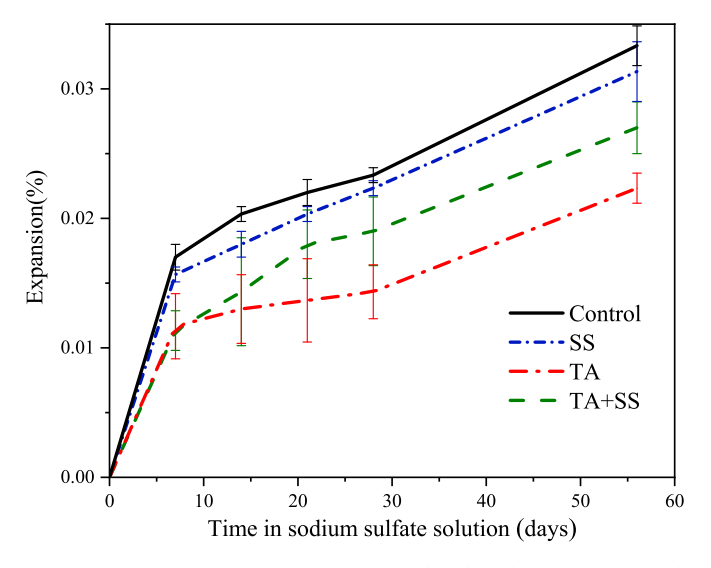


Fig. 11. Expansions of cement mortars produced with different methods immersed in 50~g/L sodium sulfate solution.

#### Data availability

Data will be made available on request.

#### Acknowledgments

The financial supports from the U.S. National Science Foundation (CMMI 1761762, ITE 2236331) and the Fundamental Research Funds for the Central Universities of Tongji University (22120230045) are highly appreciated are highly appreciated. Any opinions, findings, conclusions, or recommendations expressed in this material are those of the author(s) and do not necessarily reflect those of the National Science Foundation and National Natural Science Foundation of China.

#### References

- Y. Reches, Nanoparticles as concrete additives: review and perspectives, Construct. Build. Mater. 175 (2018) 483–495.
- [2] H. Li, H. gang Xiao, J. ping Ou, A study on mechanical and pressure-sensitive properties of cement mortar with nanophase materials, Cement Concr. Res. 34 (2004) 435–438.
- [3] Q. Ye, Z. Zhang, D. Kong, R. Chen, Influence of nano-SiO2 addition on properties of hardened cement paste as compared with silica fume, Construct. Build. Mater. 21 (2007) 539–545
- [4] U. Sharma, A. Solanki, L.P. Singh, Granulometric effect of silica nanoparticles on hydration kinetics and microstructure of cement based materials, European Journal of Environmental and Civil Engineering (2022) 1–13.
- [5] I. Flores, K. Sobolev, L.M. Torres-Martinez, E.L. Cuellar, P.L. Valdez, E. Zarazua, Performance of cement systems with nano-SiO2 particles produced by using the sol-gel method, Transport. Res. Rec. (2010) 2141.
- [6] L.P. Singh, D. Ali, U. Sharma, Studies on optimization of silica nanoparticles dosage in cementitious system, Cem. Concr. Compos. 70 (2016).
- [7] T.M. Mendes, D. Hotza, W.L. Repette, Nanoparticles in cement based materials: a review, Rev. Adv. Master. Sci. 40 (2015) 89–96.
- [8] E. Ghafari, H. Costa, E. Júlio, A. Portugal, L. Durães, The effect of nanosilica addition on flowability, strength and transport properties of ultra high performance concrete, Mater. Des. 59 (2014) 1–9.
- [9] H. Li, H.G. Xiao, J. Yuan, J. Ou, Microstructure of cement mortar with nanoparticles, Compos. B Eng. 35 (2004) 185–189.
- [10] A.H. Korayem, N. Tourani, M. Zakertabrizi, A.M. Sabziparvar, W.H. Duan, A review of dispersion of nanoparticles in cementitious matrices: nanoparticle geometry perspective, Construct. Build. Mater. 153 (2017) 346–357.
- [11] K. Sato, J.G. Li, H. Kamiya, T. Ishigaki, Ultrasonic dispersion of TiO2 nanoparticles in aqueous suspension, J. Am. Ceram. Soc. 91 (2008) 2481–2487.
- [12] A.E. Hagerman, K.M. Riedl, G.A. Jones, K.N. Sovik, N.T. Ritchard, P.W. Hartzfeld, T.L. Riechel, High molecular weight plant polyphenolics (tannins) as biological antioxidants, J. Agric. Food Chem. 46 (1998) 1887–1892.
- [13] T.S. Sileika, D.G. Barrett, R. Zhang, K.H.A. Lau, P.B. Messersmith, Colorless multifunctional coatings inspired by polyphenols found in tea, chocolate, and wine, Angew. Chem. Int. Ed. 52 (2013) 10766–10770.
- [14] X. Qian, J. Wang, L. Wang, Y. Fang, P. Chen, M. Li, A clean dispersant for nanosilica to enhance the performance of cement mortars, J. Clean. Prod. 371 (2022), 133647.
- [15] Y. Fang, J. Wang, X. Qian, L. Wang, P. Chen, P. Qiao, A renewable admixture to enhance the performance of cement mortars through a pre-hydration method, J. Clean. Prod. 332 (2021).

- [16] L. Wang, J. Wang, X. Qian, Y. Fang, P. Chen, A. Tuinukuafe, Tea stain-inspired treatment for fine recycled concrete aggregates, Construct. Build. Mater. 262 (2020), 120027.
- [17] M. Theobald, J. Plank, C-S-H-Polycondensate nanocomposites as effective seeding materials for Portland composite cements, Cem. Concr. Compos. 125 (2022).
- [18] V. Kanchanason, J. Plank, Effect of calcium silicate hydrate polycarboxylate ether (C-S-H-PCE) nanocomposite as accelerating admixture on early strength enhancement of slag and calcined clay blended cements, Cement Concr. Res. 119 (2019) 44–50
- [19] ASTM, C191-13, Standard Test Methods for Time of Setting of Hydraulic Cement by Vicat Needle, West Conshohocken, PA, 2013.
- [20] ASTM, C1437-15, Standard Test Method for Flow of Hydraulic Cement Mortar., Standard, 2015, pp. 7-8.
- [21] ASTM, C1012-15, Standard Test Method for Length Change of Hydraulic-Cement Mortars Exposed to a Sulfate Solution, West Conshohocken, PA, 2015.
- [22] Z. Gao, I. Zharov, Large pore mesoporous silica nanoparticles by templating with a nonsurfactant molecule, tannic acid, Chem. Mater. 26 (2014) 2030–2037.
- [23] D. Kong, G. He, H. Pan, Y. Weng, N. Du, J. Sheng, Influences and mechanisms of Nano-C-S-H gel addition on fresh properties of the cement-based materials with sucrose as retarder, Materials 13 (2020).
- [24] J. Wu, Y.J. Zhu, F. Chen, X.Y. Zhao, J. Zhao, C. Qi, Amorphous calcium silicate hydrate/block copolymer hybrid nanoparticles: synthesis and application as drug carriers, Dalton Trans. 42 (2013) 7032–7040.
- [25] Y. Fang, J. Wang, X. Qian, L. Wang, Y. Dong, P. Qiao, Low-cost, ubiquitous biomolecule as a strength enhancer for cement mortars, Construct. Build. Mater. 311 (2021), 125305.
- [26] D.P. Bentz, Lithium, potassium and sodium additions to cement pastes, Adv. Cement Res. 18 (2006) 65–70.
- [27] H. Justnes, E.C. Nygaard, Technical calcium nitrate as set accelerator for cement at low temperatures, Cement Concr. Res. 25 (1995) 1766–1774.
- [28] L. Wang, D. Zheng, S. Zhang, H. Cui, D. Li, Effect of nano-SiO2 on the hydration and microstructure of Portland cement, Nanomaterials 6 (2016) 241.
- [29] M. Aly, M.S.J. Hashmi, A.G. Olabi, M. Messeiry, E.F. Abadir, A.I. Hussain, Effect of colloidal nano-silica on the mechanical and physical behaviour of waste-glass cement mortar, Mater. Des. 33 (2012) 127–135.
- [30] R. Yu, P. Spiesz, H.J.H. Brouwers, Effect of nano-silica on the hydration and microstructure development of Ultra-High Performance Concrete (UHPC) with a low binder amount, Construct. Build. Mater. 65 (2014) 140–150.
- [31] F. Karagöl, R. Demirboğa, M.A. Kaygusuz, M.M. Yadollahi, R. Polat, The influence of calcium nitrate as antifreeze admixture on the compressive strength of concrete exposed to low temperatures, Cold Reg. Sci. Technol. 89 (2013) 30–35.
- [32] P. Hou, S. Kawashima, K. Wang, D.J. Corr, J. Qian, S.P. Shah, Effects of colloidal nanosilica on rheological and mechanical properties of fly ash–cement mortar, Cem. Concr. Compos. 35 (2013) 12–22.
- [33] Y. Fang, J. Wang, H. Ma, L. Wang, X. Qian, P. Qiao, Performance enhancement of silica fume blended mortars using bio-functionalized nano-silica, Construct. Build. Mater. 312 (2021), 125467.
- [34] L. Alarcon-Ruiz, G. Platret, E. Massieu, A. Ehrlacher, The use of thermal analysis in assessing the effect of temperature on a cement paste, Cement Concr. Res. 35 (2005) 609–613.
- [35] Q. Zhou, F.P. Glasser, Thermal stability and decomposition mechanisms of ettringite at <120°C, Cement Concr. Res. 31 (2001) 1333–1339.</p>
- [36] H. Van Damme, Concrete material science: past, present, and future innovations, Cement Concr. Res. 112 (2018) 5–24.
- [37] H. Zhang, W. Wang, Q. Li, Q. Tian, L. Li, J. Liu, A starch-based admixture for reduction of hydration heat in cement composites, Construct. Build. Mater. 173 (2018) 317–322.